Published in final edited form as:

J Cell Physiol. 2020 May ; 235(5): 4655–4666. doi:10.1002/jcp.29343.

Podosome Formation Impairs Endothelial Barrier Function by Sequestering Zonula Occludens Proteins

Yan-Ning Rui[1], **Yawen Chen**[1,2], **Yichen Guo**[1,2], **Caroline E. Bock**[1], **John P. Hagan**[1], **Dong H. Kim**[1,#], **Zhen Xu**[1,#]

[1]Department of Neurosurgery, McGovern Medical School, The University of Texas Health Science Center at Houston, Houston, TX 77030 U.S.A.

[2]Department of Neurology, The First Affiliated Hospital of Xi'an Jiaotong University, Xi'an, Shaanxi, China.

Abstract

Podosomes and tight junctions are subcellular compartments that both exist in endothelial cells and localize at cell surfaces. In contrast to the well-characterized role of tight junctions in maintaining cerebrovascular integrity, the specific function of endothelial podosomes remains unknown. Intriguingly, we discovered cross-talk between podosomes and tight junctions in human brain endothelial cells. Tight junction scaffold proteins ZO-1 and ZO-2 localize at podosomes in response to phorbol-12-myristate-13-acetate (PMA) treatment. We found that both ZO proteins are essential for podosome formation and function. Rather than being derived from new protein synthesis, podosomal ZO-1 and ZO-2 are relocated from a pre-existing pool found at the peripheral plasma membrane with enhanced physical interaction with cortactin, a known protein marker for podosomes. Sequestration of ZO proteins in podosomes weakens tight junction complex formation, leading to increased endothelial cell permeability. This effect can be further attenuated by podosome inhibitor PP2. Altogether, our data revealed a novel cellular function of podosomes, specifically, their ability to negatively regulate tight junction and endothelial barrier integrity, which have been linked to a variety of cerebrovascular diseases.

Keywords

Podosome; endothelial barrier; tight junction; cerebrovascular disease; cortactin; ZO-1; ZO-2

[#]Corresponding author: Zhen.Xu@uth.tmc.edu; Dong.H.Kim@uth.tmc.edu.

Author Contribution Statement

Z.X. and D.H.K. conceived and designed the experiments. Y.N.R. carried out most of the experiments. Y.G., Y.C. and C.B. performed DNA cloning and qRT-PCR. J.P.H edited the manuscript. Y.N.R. and Z.X. analyzed the experimental data and wrote the manuscript.

Conflict of Interest Statement

The authors have no conflicts to disclose.

Data Availability Statement

The data that support the findings of this study are available from the corresponding author upon reasonable request.

Introduction

Vascular endothelial cells lining the inner surface of blood vessels serve as a barrier that separates blood fluid and surrounding tissues. It is well known that the endothelial barrier is semi-permeable, so that the fluids and nutrients in the blood, as well as the waste products generated by the tissues, can be exchanged in a selective manner (Rahimi, 2017). To maintain selectivity, a variety of signaling cues, such as vascular endothelial growth factor (VEGF), transforming growth factor β (TGF-β), and intracellular protein kinases regulate the function of endothelial cells (Sukriti, Tauseef, Yazbeck, & Mehta, 2014). Dysregulated endothelial cells often cause impairment of endothelial barrier function, which has been linked to cerebrovascular diseases, such as intracranial aneurysm, subarachnoid hemorrhage, and vascular dementia (Peeyush Kumar et al., 2019; F. Wang et al., 2018; Yamamoto et al., 2017).

Over the past decade, it has been well documented that most of the signaling cues that regulate endothelial barrier function ultimately converge on three types of intercellular junctions: tight junctions, adherens junctions, and gap junctions (Bazzoni & Dejana, 2004). A tight junction (TJ) is also known as an occluding junction, which seals adjacent endothelial cells thus forming a continuous blood vessel. TJs become more prominent in the blood-brain barrier as it requires stricter control of endothelial barrier function. The blood-brain barrier is responsible for the restriction of the exchange of fluid and solutes through paracellular spaces; leakage of improper substances into the brain parenchyma often has detrimental effects (Bauer & Traweger, 2016). TJs consist of different proteins such as membrane-spanning proteins from the claudin family and scaffolding proteins from the zonula occludens (ZO) family. In endothelial cells, the amino-terminal region of ZO-1 physically interacts with claudin 5 while its carboxy-terminal domain binds to cortactin and actin, thus bridging the tight junction to intracellular cytoskeleton (Stamatovic, Johnson, Keep, & Andjelkovic, 2016). Although ZO proteins predominantly localize at cell-cell contacts, they can be redistributed to other cellular compartments such as nuclei during the wound-healing process (Gottardi, Arpin, Fanning, & Louvard, 1996). Interestingly, ZO-1 proteins reportedly localized to podosomes, another cellular compartment, in a smooth muscle cell line (Kremerskothen et al., 2011). We recently observed localization of ZO proteins to podosomes in endothelial cells, suggesting a possible role for ZO proteins in the deregulation of smooth muscle and endothelial cells, both of which can contribute to vascular disease.

A podosome is a subcellular organelle that mediates the interactions between the cell and the extracellular matrix (ECM). Among all the adhesive structures between the cell and the ECM, a podosome is quite unique due to its degradative capacity by enriching ECM-lytic enzymes (Alonso, Spuul, Daubon, Kramer, & Genot, 2019). The formation of podosomes requires actin and its regulator cortactin, both of which have been widely used as markers for the podosome (Seano, Daubon, Genot, & Primo, 2014). Many intracellular protein kinases were reported to be involved in podosome formation (Foxall, Pipili, Jones, & Wells, 2016). For instance, SRC as a non-receptor tyrosine kinase can phosphorylate cortactin at tyrosine 421 and in turn promote cortactin-mediated actin assembly in podosomes (Luxenburg, Parsons, Addadi, & Geiger, 2006; Tehrani, Tomasevic, Weed, Sakowicz, &

Cooper, 2007). Although both cortactin and actin are constituents of TJs and podosomes, it is completely unknown whether these two distinct organelles cross-talk in endothelial cells.

Our results suggested that ZO proteins including ZO-1 and ZO-2 play a critical role in the cross talk in endothelial cells. We found that both ZO-1 and ZO-2 localize to podosomes in brain endothelial cells in response to phorbol ester treatment. Podosomal ZO-1 and ZO-2 proteins are mainly contributed by a pre-existing pool found at the peripheral plasma membrane instead of new protein synthesis in the cell. Interestingly, a single knockdown of ZO-1 or ZO-2 is sufficient to block phorbol ester-induced podosome responses, including podosome formation and ECM degradation, possibly due to impaired dimerization of ZO proteins. Moreover, the endothelial barrier function is compromised when podosome formation is induced, as induced podosomes sequester dimerized ZO proteins away from the plasma membrane.

Results

Zona occludens proteins localize to podosomes in brain endothelial cells

To reveal the potential link between tight junctions and podosomes in endothelial cells, we co-immunostained the corresponding markers ZO-1 and actin, respectively. We chose primary human brain microvascular endothelial cells (HBMECs) instead of human umbilical vein endothelial cells (HUVECs) as our *in vitro* model in order to render our study more physiologically relevant to cerebrovascular diseases. As shown in Figure 1a, ZO-1 predominantly localizes at cell-cell contacts (green signals in Figure 1a2), while actin presents as stress fibers (red signals in Figure 1a3). Similar to other endothelial cells (Varon et al., 2006), HBMECs containing podosomes were infrequently detected under unstimulated conditions. Therefore, we further treated cells with phorbol-12-myristate-13-acetate (PMA), a widely-used agent that induces podosome formation in a variety of cell types (Billottet et al., 2008; Starnes, Cortesio, & Huttenlocher, 2011). Indeed, PMA treatment induces the formation of podosomes in HBMECs, some of which further assemble into a ring-like structure called a podosome rosette (indicated by white arrows in Figure 1a6). Our co-immunostaining results showed that ZO-1 largely co-localizes with actin in podosomes, as indicated by the merged yellow signals (Figure 1a4 and a7). We also found that ZO-1 is well co-localized with cortactin, another widely-used podosome marker, in response to PMA treatment (see merged yellow signals in Figure 1b4 and b7).

In addition to ZO-1, the zona occludens family has two other members, ZO-2 and ZO-3 (Bauer & Traweger, 2016). Before examining whether ZO-2 and ZO-3 also localize to podosomes, we checked their expression in HBMECs. By real-time quantitative RT-PCR, we found that the mRNA level of ZO-2 is comparable to ZO-1 while ZO-3 is barely detected (Supplemental Figure 1a). Western blotting confirmed that both ZO-1 and ZO-2 but not ZO-3 were expressed in HBMECs (Supplemental Figure 1b–d). The specificities of antibodies against ZO-1 and ZO-2 were evaluated by gene-specific knockdown using small interfering RNAs (Supplemental Figure 1c–d). In addition, the immunofluorescence specificities of these antibodies were confirmed in HBMECs (Supplementary Figure 1e–f). These data suggest that only two members of the zona occludens family, ZO-1 and ZO-2, are expressed in HBMECs. Therefore, we examined the putative co-localization between

ZO-2 and podosome markers actin and cortactin, and found results similar to those found for ZO-1 (Supplemental Figure 2). In contrast, we failed to detect the podosomal localization of claudin 5 (Supplementary Figure 3), a membrane-spanning protein found in tight junctions, suggesting that podosomes partially sequester tight junction components.

ZO-1 and ZO-2 are essential for podosome function in a non-redundant manner

To figure out the functional significance of ZO-1/2 in podosomes, we examined the *in situ* degradation of the extracellular matrix using a standard assay to evaluate the unique feature of the podosome as a degradative organelle. In brief, HBMECs are seeded onto chamber slides that are pre-coated with fluorescence-labeled gelatin, which can be degraded by podosomes and presented as a dark area. As shown in Figure 2a, PMA treatment dramatically induced gelatin degradation as indicated by dark spots (comparing Figure 2a5 to 2a1). Surprisingly, knockdown of ZO-1 or ZO-2 significantly reduces PMA-induced gelatin degradation (comparing Figure 2a6 and a7 to a5, quantification shown in Figure 2b), suggesting that both ZO-1 and ZO-2 are essential for podosome function. To reduce potential off-target effects, we repeated the experiments with another non-overlapping siRNA that targeted ZO-1 and ZO-2, respectively, producing similar results which were included in the quantifications (Figure 2b). To save limited space, an image with one of the targeted siRNAs was presented. It is worth mentioning that ZO-1 and ZO-2 are known to be redundant in tight junction formation (Umeda et al., 2006). In contrast, our results suggest a distinct mechanism for these ZO proteins in podosomes where ZO-1 and ZO-2 act in a non-redundant manner. Consistently, simultaneous knockdown of ZO-1 and ZO-2 did not lead to further reduction of PMA-induced gelatin degradation (comparing Figure 2a8 to a6 and a7, and quantification shown in Figure 2b).

Dimerization of ZO proteins is responsible for their non-redundant roles in podosomes

To dissect the molecular mechanism of ZO-mediated podosome function, we first examined the role of ZO-1 and ZO-2 in podosome formation. As shown in Figure 2c, knockdown of ZO-1 or ZO-2 attenuates PMA-induced podosome formation in HBMECs in a non-redundant pattern that is similar to how they behave in PMA-induced podosome function (Figure 2a–b). We wondered whether knockdown of one ZO member would lead to the destabilization of the other, since they form a protein complex through physical interaction (Fanning & Anderson, 2009). Interestingly, ZO-2 was stably expressed when ZO-1 was depleted in HBMECs and vice versa (Figure 3a), suggesting that the protein stability of ZO-1 and ZO-2 are not mutually dependent.

As multi-domain scaffold proteins, ZO-1 and ZO-2 form dimers mainly through the second PDZ domain (PDZ2) (Wu et al., 2007) (Supplemental Figure 4a). We wondered whether dimerization between ZO-1 and ZO-2 could contribute to their non-redundant role in podosome responses. To interfere with their dimerization ability in a dominant-negative manner, a construct that expressed the PDZ2 domain of ZO-1 was created (Supplemental Figure 4b). A protein binding competition assay was performed as previously described (David-Morrison et al., 2016). Indeed, the binding affinity between myc-tagged ZO-1 and FLAG-tagged ZO-2 was dramatically reduced when expression of the HA-tagged PDZ2 construct was increased (Figure 3b–c). Importantly, overexpression of the dimer inhibitor

attenuates PMA-induced podosome formation and extracellular matrix degradation (Figure 3d–e). Altogether, our results support the idea that the dimerization of ZO proteins plays an important role in podosome formation and function, which is consistent with their non-redundant mode of action as previously observed (Figure 2).

Podosomal ZO-1/2 relocates from plasma membrane and binds more cortactin

Next, we sought to identify the origin of podosomal ZO-1/2. To determine whether new protein synthesis contributes to their podosomal localization, we carried out a real-time quantitative RT-PCR assay. However, the mRNA level of ZO-1 did not significantly change when compared to the PMA treated control (Figure 4a), and similar results were found for ZO-2 (Supplemental Figure 5a). Consistently, the total protein level of ZO-1 and ZO-2 remain unaltered in response to PMA stimulation (the upper panel and quantification in Figure 4b and the left panel in Supplemental Figure 5b). It has been reported that ZO-2 at different subcellular compartments, such as the nucleus, can be relocated from a pre-existing pool like the peripheral plasma membrane instead of from de novo protein synthesis (Islas, Vega, Ponce, & Gonzalez-Mariscal, 2002). We speculated whether a similar mechanism exists for podosomal localization of ZO proteins in HBMECs. To test this idea, we performed a cell fractionation analysis. Interestingly, the protein amount of ZO-1 in the membrane fraction of HBMECs was reduced in response to PMA treatment (left two panels and the first bar graph in Figure 4c, and ZO-1 was normalized to endothelial cell membrane-specific marker VE-cadherin). Consistently, ZO-1 protein level in the cytosolic pool was increased when HBMECs were treated by PMA (right two panels and the second bar graph in Figure 4c, and ZO-1 was normalized to cytosolic marker Hsp90). We also examined ZO-2 and found similar results (Supplemental Figure 5b). Altogether, these results strongly support that the localization of ZO-1/2 to podosomes originates from a pre-existing pool in the plasma membrane, and not from de novo protein synthesis.

As a scaffold protein, ZO-1/2 binds to different partners in a domain-dependent manner. The amino-terminal of ZO-1/2 interacts with the cytoplasmic tail of claudin 5, while its carboxyl-terminal binds to cortactin and actin (Bazzoni & Dejana, 2004). To figure out whether their binding partners are involved in the relocation of ZO proteins into podosomes, we analyzed their physical interaction in response to PMA treatment. As shown in Figure 5a, in comparison to the negative controls, the co-immunoprecipitated claudin 5 is drastically reduced when HBMECs are stimulated by PMA (see the first row), suggesting that a dissociation occurs between ZO-1 and claudin 5. Interestingly, the physical interaction between ZO-1 and cortactin is significantly enhanced while the binding of ZO-1 to actin was not affected (Figure 5b–c), indicating that cortactin is involved in the redistribution of ZO-1 at a subcellular level. Given cortactins importance in podosome assembly, we also examined the physical interaction between ZO-1 and phosphorylated cortactin, which can be induced by SRC kinase at its tyrosine 421 (Luxenburg et al., 2006). Our data showed that PMA treatment increases their binding affinity (Figure 5d), suggesting that ZO-1 has a higher affinity to a phosphorylated form of cortactin that is often induced by podosome activation signals. Similar results were found for the binding affinity between ZO-2 and cortactin or p-Y421-cortactin in HBMECs (Supplemental Figure 6).

Sequestration of ZO proteins in podosomes impairs endothelial barrier function

As a scaffold protein for tight junction, ZO-1/2 is swiftly recruited to podosomes in response to PMA treatment. Therefore, the endothelial barrier may be weakened accordingly. To examine this, we carried out two different assays which included assessing *in vitro* vascular endothelial permeability and endothelial gap formation. For the endothelial permeability assay, brain endothelial cells were implanted onto the upper membrane of the two chamber insert and grown to full confluence. FITC-dextran, a fluorescent-labeled large molecule that is normally not able to pass through the confluent monolayer of endothelial cells, is added to the upper chamber in order to monitor the potential leakiness induced by various stimulations. Different from the tracer-based leakage assay, the endothelial gap formation assay is another independent, image-based approach which quantifies gap areas highlighted by VE-cadherin in endothelial cells (Aragon-Sanabria et al., 2017; Y. Wang & Alexander, 2011). As shown in Figure 6a–b, PMA treatment significantly increases the penetration of FITC-dextran and the percentage of the endothelial gap, respectively, suggesting when PMA induces podosome formation, endothelial barrier function is also impaired.

To demonstrate the role of podosome formation in PMA-induced endothelial barrier leakage, we further treated HBMECs with PP2, a well-known SRC kinase inhibitor that blocks podosome formation (J. Wang et al., 2009). As expected, PP2 treatment inhibits PMA-induced SRC activation, judging by the level of the active form of SRC (p-Y416-SRC) (Figure 6c). Moreover, PP2 treatment attenuated PMA-induced binding affinity between ZO-1 and cortactin or p-Y421-cortactin (Figure 6d), possibly by reducing the amount of SRC-mediated phosphorylated cortactin. Importantly, PMA-induced endothelial permeability and gap formation in HBMECs were significantly improved by PP2 treatment (Figure 6e–f), suggesting that podosome formation negatively regulates endothelial barrier function.

Vascular endothelial growth factor (VEGF) similarly regulates podosomal ZO proteins

To investigate whether other physiological cues also regulate localization and function of ZO proteins in podosomes, we treated HBMECs with VEGF, a ligand existing in the blood circulatory system. As shown in Figure 7a–b, VEGF treatment induced both podosome formation and ECM degradation. Importantly, both ZO-1 and ZO-2 relocated into podosomes upon VEGF stimulation (Figure 7c and Supplemental Figure 7). To evaluate the effects of VEGF treatment and the potential role of podosomes on endothelial barrier function, we performed both the FITC-dextran permeability and endothelial gap formation assays with and without SRC inhibitor. Consistent with other reports, VEGF treatment disrupts endothelial barrier function (Figure 7d–e) and further PP2 treatment rescued the defects (Figure 7f–g), suggesting that VEGF-induced podosome activity is critically involved.

To summarize the aforementioned findings, we proposed a schematic model as illustrated in Figure 7h. On the left side, podosomes contain an actin-enriched core together with other regulators such as cortactin (indicated by filled circle in light green). As for the tight junction shown on the right side, ZO-1/2 forms dimers and interacts with membrane-spanning proteins claudin and cortactin, thus bridging the tight junction to cytoskeleton.

Following podosome induction by phorbol ester or VEGF, ZO-1/2 relocates from tight junctions at the plasma membrane into podosomes (as indicated by the double-headed arrow in black), likely due to the enhanced physical interaction between ZO-1/2 and cortactin. On one hand, the dissociation between ZO-1/2 and claudin weakens the intercellular junction. On the other hand, podosomal ZO-1/2 facilitate cortactin-mediated actin assembly, which further recruits membrane-type metalloprotease MT1-MMP. MT1-MMP activates MMP2 for ECM degradation. Notably, MMP9, another member of MMP detected in podosomes in other cell types, is not included in our model since our preliminary data excluded its presence in HBMECs. Our model supports the notion that podosome formation impairs endothelial barrier function by sequestration of ZO-1/2, a finding that may provide insight into many types of cerebrovascular diseases that are related to blood-brain barrier dysfunction.

Discussion

Podosome formation negatively regulates TJ.

It is well documented that podosomes recruit metalloproteases for efficient degradation of the extracellular matrix. Our data revealed a novel cellular effect elicited by podosome formation, i.e., negative regulation of TJs. As demonstrated in Figure 6e–f, when podosome formation is induced by PMA, an activator of protein kinase C, both ZO-1 and ZO-2 can be sequestered to podosomes, which further compromises endothelial barrier function. In additional to the activation of protein kinase C, we found VEGF, a physiologically existing ligand, regulates ZO proteins in podosomes in a similar manner (Figure 7a–g). These observations may suggest a unifying mechanism of cross-talk between podosomes and tight junctions under different stresses. It is possible that VEGF serves as the upstream signal of protein kinase C, which has been reported in several other cell lines (Jiang, Qin, & Han, 2016; Lin et al., 2018).

Generally, in the absence of stimuli, including the treatment of PMA or the aforementioned growth factors, ZO proteins predominantly locate at cell-cell points of contact (Figure 1 and Supplemental Figure 2). However, they do relocate to other cellular compartments under stress conditions. For instance, ZO-1 is enriched in the nucleus during remodeling of cell-cell contacts (Gottardi et al., 1996). It can bind to the transcription factor ZONAB and activate the expression of ErbB-2 in epithelial cells (Balda & Matter, 2000). Our study revealed for the first time that the podosome can act as another subcellular compartment for ZO proteins in endothelial cells. Importantly, both ZO-1 and ZO-2 are essential for podosome formation and function (Figure 2 and Figure 3a). We noticed that PMA treatment has a negligible effect on the intensity of ZO proteins in the nucleus (Figure 1 and supplemental Figure 2), suggesting that their redistribution into the podosome or nucleus can be mediated by distinct mechanisms in response to different stresses.

Sequestration of ZO proteins in podosomes weakens TJs and leads to defective endothelial barriers (Figure 6 and 7). In addition, other types of intercellular junctions, such as the adherens junction, also regulate endothelial barrier function (Dejana, Orsenigo, & Lampugnani, 2008). In endothelial cells, adherens junctions comprise membrane-spanning proteins including VE-cadherin, nectin, and PECAM, and their associated adaptor proteins,

including p120-catenin, β-catenin, and plakoglobin (Dejana & Orsenigo, 2013). It will be interesting to see whether podosome formation has a similar effect on adherens junctions, such as the sequestration of their adaptor proteins. Prior evidence has suggested such a possibility wherein p120-catenin was found to physically interact with cortactin (Boguslavsky et al., 2007). More experiments in the future are required to clarify this speculation.

A novel mechanism for ZO-mediated podosome formation and function

As scaffold proteins, ZO-1 and ZO-2 have multiple domains including PDZ, Guanylate kinase-like domain (GK), and SH3 domains (Supplemental Figure 4a) (Fanning & Anderson, 2009). It has been reported that ZO-1 and ZO-2 compensate each other in TJ assembly (Umeda et al., 2006). In contrast, our results demonstrated that their function in podosomes is non-redundant (Figure 2). Utilizing a dominant-negative mutant that expresses the second PDZ domain of ZO-1, we showed that the dimerization of ZO proteins is critically involved in podosome formation and function (Figure 3c–e). It is well known that ZO-1 and ZO-2 form heterodimers *in vitro* and *in vivo* (Odenwald et al., 2018; Wu et al., 2007), although their homodimerization remains controversial (Fanning, Jameson, Jesaitis, & Anderson, 1998). Some of our evidence favors the notion that heterodimerization of ZO-1 and ZO-2 is important for their roles in podosomes. For example, single knockdowns of ZO-1 or ZO-2 blocks podosome formation and function (Figure 2), suggesting that the remaining homodimers of ZO-1 or ZO-2, even if they exist abundantly, are insufficient or nonfunctional. In addition, double knockdown of ZO-1 and ZO-2 does not show any additive effects on podosome responses in comparison with the single knockdown (Figure 2a), likely due to the saturated loss of heterodimers in either condition. Moreover, overexpression of the PDZ2 domain dramatically reduces the binding affinity between ZO-1 and ZO-2, and inhibits podosome formation and ECM degradation (Figure 3d–e). It is worth mentioning that ZO-1 and ZO-2 knockout mice are both embryonically lethal (Katsuno et al., 2008; Xu et al., 2008), a fact that cannot be explained by their redundant role in TJs. Based on our study, it is reasonable to postulate that podosome defects may contribute to the non-redundant role of ZO proteins in mouse development.

As for the relocation mechanism of ZO-1 and ZO-2 from the peripheral plasma membrane to podosomes in endothelial cells, our data suggests that cortactin plays an important role. For example, we observed the binding affinity between ZO-1 and a phosphorylated form of cortactin to be enhanced (Figure 5d). Interestingly, this phosphorylation site is mainly activated by SRC kinase (Luxenburg et al., 2006; Tehrani et al., 2007), which localizes at both tight junctions and podosomes. We speculate that SRC near tight junctions may promote the interaction between cortactin and ZO proteins by phosphorylating cortactin at Y421. Alternatively, the ZO-cortactin complex may initially shuttle into pre-podosomal sites before cortactin gets phosphorylated by SRC that is nearby podosomes. To distinguish these two possibilities, analyses on the localized SRC activity will be helpful. It is worth noting that in other cell types, such as smooth muscle cells, ZO-1 was also found to localize to podosomes with the aid of actin but not cortactin (Kremerskothen et al., 2011), implying that the molecular mechanism for the redistribution of ZO proteins might be cell type-specific.

Our study ultimately revealed a novel role of podosomes in tight junction stability that is essential for endothelial barrier function. Mechanistically, podosome sequesters ZO-1 and ZO-2, which form dimers and have higher binding affinity with SRC-phosphorylated cortactin. Consistently, inhibiting SRC activity by PP2 treatment efficiently attenuated PMA-induced endothelial barrier leakiness. As such, the podosome may emerge as a novel therapeutic target for preventing endothelial barrier dysfunction that has been linked to various cerebrovascular diseases.

Materials and Methods

Cell culture, transfection and stimulation

Human brain microvascular endothelial cells (HBMECs) were purchased from Cell Systems (ACBRI 376) and maintained in endothelial cell medium (#1001, ScienCell Research Laboratories). Transfections of plasmid DNA were performed using lipofectamine 3000 (Invitrogen) according to manufacturer's instructions. Small interfering RNAs were introduced into HBMECs by standard electroporation protocol (Neon® Transfection System, Invitrogen). To induce podosome formation, phorbol-12-myristate-13-acetate (PMA) was added to HBMECs to a final concentration of 100 nM for 1 hour followed by different assays such as immunostainings, *in situ* extracellular matrix degradation, and *in vitro* endothelial cell permeability. Similarly, VEGF (50 ng/ml, 1 hour) was used to treat HBEMCs to induce podosome formation and function. PP2 (10 μM, 1 hour) was used to inhibit endogenous SRC kinase activity.

DNA cloning

Full length myc-tagged ZO-1 and FLAG-tagged ZO-2 are available from addgene (#30317 and # 27415, respectively). The PDZ2 domain of ZO-1 (nucleotide 514–753) was sub-cloned into pCMV5 by standard PCR protocol and verified by Sanger sequencing as we previously performed (Y. N. Rui et al., 2017).

SiRNA

Stealth small interfering RNAs against human ZO-1 and ZO-2 were purchased from Invitrogen (TJP1HSS110773 and TJP1HSS110774 for ZO-1; TJP2HSS113980 and TJP2HSS113982 for ZO-2). The knockdown efficiency of each siRNA was validated by Western blotting.

Quantitative RT-PCR

Total mRNA level of ZO-1, ZO-2 and ZO-3 were isolated from HBEMCs by TRIzol and quantitatively detected based on the SYBR green protocol (4309155, ThermoFisher Scientific). The primers used are listed as follows:

ZO-1: 5'-AGAGTGGTTCTTCGAGAAGCTGGA/5'-CGTCTCGTGGTTCACTCTTTGCAA

ZO-2: 5'-GGAGCATTGACCAGGACTACGAG/5'-AGCCGGAGACCATACTCTTCGT

ZO-3: 5’-AGTGGTGTTGCGAGAAGCCAG /5’-TTCAGAGGGATGGTGGCTGTG

Antibody

ZO-1 (13663), ZO-2 (2847), ZO-3 (3704), cortactin (3503), p-Y421-cortactin (4569), Hsp90 (4877), VE-cadherin (2500), SRC (2108), p-Y416-SRC (6943) from Cell Signaling Technology; Claudin 5 (ab15106, Abcam); Actin (MAB1501, EMD Millipore); GAPDH (sc-32233) and Myc (sc-40) from Santa Cruz Technology; FLAG (MAB3118, Sigma-Aldrich); HA (11583816001, Roche).

Western blotting

Transiently transfected HBMECs or HEK293T cells in 60-mm dishes were lysed in a Triton X-100 lysis buffer as previously described (Y. N. Rui et al., 2015) and sonicated briefly before centrifugation at 13,000 rpm for 30 min at 4 °C. Total cell lysates were added by 2X SDS sample buffer and then subjected to SDS-PAGE analysis. Proteins were transferred to nitro-cellulose membranes using Bio-Rad mini transfer apparatus followed by blocking with 5% non-fat milk. Primary antibodies and secondary antibodies were generally used at 1:1000 and 1:10000 dilutions respectively before using the LI-COR Odyssey system to detect fluorescence signals. The number value of each Western band was measured by Image Studio Lite associated with the Odyssey system. After being normalized to loading controls GAPDH, VE-cadherin, or HSP90, the fold change of the protein of interest is presented in a bar graph. Data were reported as mean ± s.e.m. (n=3 independent experiments).

Co-Immunoprecipitation/Co-IP

Transiently transfected HBMECs or HEK293T cells in 60-mm dishes were lysed in an IP-lysis buffer as previously described (Y. Rui et al., 2004) and sonicated briefly before centrifugation at 13,000 rpm for 30 min at 4°C. Endogenous ZO-1 or HA-tagged ZO-1 was immunoprecipitated from the cell lysate with anti-ZO-1 or anti-HA antibody plus protein A/G Plus agarose beads (Santa Cruz Biotechnology, sc-2003). Immunoprecipitates or whole cell lysates (WCL) were subjected to standard Western blotting.

Immunostaining

HBMECs were re-seeded onto 8-well chamber slides and stimulated by PMA (100 nM) for 1 hour before 4% paraformaldehyde fixation. Fixed cells were blocked in 10% normal goat serum at room temperature for 1 hour followed by incubation in primary antibodies at 4°C overnight, and then stained with Alexa-594 or Alexa-488 conjugated secondary antibodies (Invitrogen). Washed samples were mounted in prolong gold solution (Invitrogen). Images were captured by Leica TCS SP5 Confocal Microscope.

Podosome formation assay

Podosome formation in HBMECs was induced by PMA treatment (100 nM for 1 hour). Cells were fixed in 4% paraformaldehyde and stained with phalloidin-Alexa597 or anti-cortactin antibody to reveal the subcellular localization of podosomes. The percentage of

cells showing podosomes with or without treatment was calculated from at least 6 different fields (×10 objective lens) per coverslip (n=3 independent experiments).

In situ extracellular matrix degradation assay

Eight-well chamber slides were sequentially treated by poly-L-lysine, glutaraldehyde, and Oregon-Green-488-conjugated gelatin as instructed (ECM670, Millipore). After washing with PBS, coverslips were disinfected by 70% ethanol. To quench residual free aldehydes, growth media was added to each well at room temperature for 30 min before cell seeding. HBMECs treated with siRNAs were grown on above pre-coated chamber slides and incubated for 12 hours before treated with PMA (100 nM, 1 hour). After fixation, the degradation of extracellular matrix was imaged by Leica DM4000 microscope. At least 9 different fields (×10 objective lens) per coverslip were selected for quantification using Image J software. The degradation index is presented as the average degradation area per cell (μm^2/cell) (n=3 independent experiments).

Membrane protein extraction

HBMECs in 60 mm dish were washed by Cell Wash Solution (provided by Mem-PER™ Plus Membrane Protein Extraction Kit, Catalog number 89842, ThermoFisher Scientific) and then lysed in Permeabilization Buffer for 10 min at 4°C with constant mixing. Lysed cells were centrifuged at top speed for 15 min. The supernatant contains cytosolic proteins while the pellet is enriched with membrane proteins, which can be further extracted by Solubilization Buffer. Both extracted supernatants will be treated by 2X SDS sample buffer before application to Western blotting analysis.

In vitro endothelial cell permeability

HBMECs were seeded onto the upper chamber of the 24-well insert (662630, Greiner bio-one) and cultured in endothelial cell media. According to manufacturer's instructions, HBEMCs were grown to full confluency and treated by podosome-inducing agent PMA (100 nM, 1 hour) and/or SRC inhibitor PP2 (10 μM, 1 hour). Media is then carefully removed and FITC-dextran (70 kd) is added and incubated for 20 min at room temperature. Equal volume of media is taken in each well containing FITC-dextran that crossed the monolayer and its amount is measured based on the absorbance of 535 nm. The fold change is calculated by normalizing the amount of FITC-dextran in each well to that under the control treatment (DMSO) (n=3 independent experiments).

Endothelial gap formation assay

HBMECs were cultured in 8-well chamber slides until full confluency. Either PMA (100 nM, 1 hour) or VEGF (50 ng/ml, 1 hour) was added to the cells in comparison with control treatment (DMSO). HBMECs were fixed in 4% formaldehyde for 15 min at room temperature followed by 0.2% Triton X-100 permeabilization in PBS for 10 min. After blocking in 5% goat serum, primary antibody against VE-cadherin (ab33168, Abcam) was added and incubated overnight at 4 °C. Cells were then washed three times in PBS and incubated with a rabbit Alexa-594 secondary antibody followed by mounting. At least 9 different fields for each sample were obtained by Leica confocal microscope. Endothelial

gap areas were identified and measured by Image J software (provided by NIH). The percentage of endothelial gap was calculated as the area not covered by HBMECs (gaps) divided by the total area of each image. Data were reported as the mean ± s.e.m. (n=3).

Statistics analysis

Statistical analysis was performed with Microsoft Excel or GraphPad Prism 5 and p-values were calculated by the Student's t-test or one-way ANOVA where Bonferroni correction is used for multiple comparison test between selected pairs. Data are represented as mean ± s.e.m. $p<0.05$ is considered significant.

Supplementary Material

Refer to Web version on PubMed Central for supplementary material.

Funding Statement and Acknowledgement

We appreciate the critical reading of this manuscript by Dr. Joanna O'Leary. The project was supported in part by RO1NS104280 and R21NS108310 grants from the US National Institutes of Health.

References

Alonso F, Spuul P, Daubon T, Kramer I, & Genot E (2019). Variations on the theme of podosomes: A matter of context. Biochim Biophys Acta Mol Cell Res, 1866(4), 545–553. doi:10.1016/j.bbamcr.2018.12.009 [PubMed: 30594495]

Aragon-Sanabria V, Pohler SE, Eswar VJ, Bierowski M, Gomez EW, & Dong C (2017). VE-Cadherin Disassembly and Cell Contractility in the Endothelium are Necessary for Barrier Disruption Induced by Tumor Cells. Sci Rep, 7, 45835. doi:10.1038/srep45835 [PubMed: 28393886]

Balda MS, & Matter K (2000). The tight junction protein ZO-1 and an interacting transcription factor regulate ErbB-2 expression. EMBO J, 19(9), 2024–2033. doi:10.1093/emboj/19.9.2024 [PubMed: 10790369]

Bauer H, & Traweger A (2016). Tight Junctions of the Blood-Brain Barrier - A Molecular Gatekeeper. CNS Neurol Disord Drug Targets, 15(9), 1016–1029. [PubMed: 27633783]

Bazzoni G, & Dejana E (2004). Endothelial cell-to-cell junctions: molecular organization and role in vascular homeostasis. Physiol Rev, 84(3), 869–901. doi:10.1152/physrev.00035.2003 [PubMed: 15269339]

Billottet C, Rottiers P, Tatin F, Varon C, Reuzeau E, Maitre JL, … Genot E (2008). Regulatory signals for endothelial podosome formation. Eur J Cell Biol, 87(8–9), 543–554. doi:10.1016/j.ejcb.2008.02.006 [PubMed: 18397815]

Boguslavsky S, Grosheva I, Landau E, Shtutman M, Cohen M, Arnold K, … Bershadsky A (2007). p120 catenin regulates lamellipodial dynamics and cell adhesion in cooperation with cortactin. Proc Natl Acad Sci U S A, 104(26), 10882–10887. doi:10.1073/pnas.0702731104 [PubMed: 17576929]

David-Morrison G, Xu Z, Rui YN, Charng WL, Jaiswal M, Yamamoto S, … Bellen HJ (2016). WAC Regulates mTOR Activity by Acting as an Adaptor for the TTT and Pontin/Reptin Complexes. Dev Cell, 36(2), 139–151. doi:10.1016/j.devcel.2015.12.019 [PubMed: 26812014]

Dejana E, & Orsenigo F (2013). Endothelial adherens junctions at a glance. J Cell Sci, 126(Pt 12), 2545–2549. doi:10.1242/jcs.124529 [PubMed: 23781019]

Dejana E, Orsenigo F, & Lampugnani MG (2008). The role of adherens junctions and VE-cadherin in the control of vascular permeability. J Cell Sci, 121(Pt 13), 2115–2122. doi:10.1242/jcs.017897 [PubMed: 18565824]

Fanning AS, & Anderson JM (2009). Zonula occludens-1 and -2 are cytosolic scaffolds that regulate the assembly of cellular junctions. Ann N Y Acad Sci, 1165, 113–120. doi:10.1111/j.1749-6632.2009.04440.x [PubMed: 19538295]

Fanning AS, Jameson BJ, Jesaitis LA, & Anderson JM (1998). The tight junction protein ZO-1 establishes a link between the transmembrane protein occludin and the actin cytoskeleton. J Biol Chem, 273(45), 29745–29753. [PubMed: 9792688]

Foxall E, Pipili A, Jones GE, & Wells CM (2016). Significance of kinase activity in the dynamic invadosome. Eur J Cell Biol, 95(11), 483–492. doi:10.1016/j.ejcb.2016.07.002 [PubMed: 27465307]

Gottardi CJ, Arpin M, Fanning AS, & Louvard D (1996). The junction-associated protein, zonula occludens-1, localizes to the nucleus before the maturation and during the remodeling of cell-cell contacts. Proc Natl Acad Sci U S A, 93(20), 10779–10784. [PubMed: 8855257]

Islas S, Vega J, Ponce L, & Gonzalez-Mariscal L (2002). Nuclear localization of the tight junction protein ZO-2 in epithelial cells. Exp Cell Res, 274(1), 138–148. doi:10.1006/excr.2001.5457 [PubMed: 11855865]

Jiang M, Qin C, & Han M (2016). Primary breast cancer induces pulmonary vascular hyperpermeability and promotes metastasis via the VEGF-PKC pathway. Mol Carcinog, 55(6), 1087–1095. doi:10.1002/mc.22352 [PubMed: 26152457]

Katsuno T, Umeda K, Matsui T, Hata M, Tamura A, Itoh M, … Tsukita S (2008). Deficiency of zonula occludens-1 causes embryonic lethal phenotype associated with defected yolk sac angiogenesis and apoptosis of embryonic cells. Mol Biol Cell, 19(6), 2465–2475. doi:10.1091/mbc.E07-12-1215 [PubMed: 18353970]

Kremerskothen J, Stolting M, Wiesner C, Korb-Pap A, van Vliet V, Linder S, … Pavenstadt H (2011). Zona occludens proteins modulate podosome formation and function. FASEB J, 25(2), 505–514. doi:10.1096/fj.10-155598 [PubMed: 20930113]

Lin CM, Titchenell PM, Keil JM, Garcia-Ocana A, Bolinger MT, Abcouwer SF, & Antonetti DA (2018). Inhibition of Atypical Protein Kinase C Reduces Inflammation-Induced Retinal Vascular Permeability. Am J Pathol, 188(10), 2392–2405. doi:10.1016/j.ajpath.2018.06.020 [PubMed: 30220554]

Luxenburg C, Parsons JT, Addadi L, & Geiger B (2006). Involvement of the Src-cortactin pathway in podosome formation and turnover during polarization of cultured osteoclasts. J Cell Sci, 119(Pt 23), 4878–4888. doi:10.1242/jcs.03271 [PubMed: 17105771]

Odenwald MA, Choi W, Kuo WT, Singh G, Sailer A, Wang Y, … Turner JR (2018). The scaffolding protein ZO-1 coordinates actomyosin and epithelial apical specializations in vitro and in vivo. J Biol Chem, 293(45), 17317–17335. doi:10.1074/jbc.RA118.003908 [PubMed: 30242130]

Peeyush Kumar T, McBride DW, Dash PK, Matsumura K, Rubi A, & Blackburn SL (2019). Endothelial Cell Dysfunction and Injury in Subarachnoid Hemorrhage. Mol Neurobiol, 56(3), 1992–2006. doi:10.1007/s12035-018-1213-7 [PubMed: 29982982]

Rahimi N (2017). Defenders and Challengers of Endothelial Barrier Function. Front Immunol, 8, 1847. doi:10.3389/fimmu.2017.01847 [PubMed: 29326721]

Rui Y, Xu Z, Lin S, Li Q, Rui H, Luo W, … Lin S C. (2004). Axin stimulates p53 functions by activation of HIPK2 kinase through multimeric complex formation. EMBO J, 23(23), 4583–4594. doi:10.1038/sj.emboj.7600475 [PubMed: 15526030]

Rui YN, Xu Z, Fang X, Menezes MR, Balzeau J, Niu A, … Kim DH (2017). The Intracranial Aneurysm Gene THSD1 Connects Endosome Dynamics to Nascent Focal Adhesion Assembly. Cell Physiol Biochem, 43(6), 2200–2211. doi:10.1159/000484298 [PubMed: 29069646]

Rui YN, Xu Z, Patel B, Chen Z, Chen D, Tito A, … Zhang S (2015). Huntingtin functions as a scaffold for selective macroautophagy. Nat Cell Biol, 17(3), 262–275. doi:10.1038/ncb3101 [PubMed: 25686248]

Seano G, Daubon T, Genot E, & Primo L (2014). Podosomes as novel players in endothelial biology. Eur J Cell Biol, 93(10–12), 405–412. doi:10.1016/j.ejcb.2014.07.009 [PubMed: 25199436]

Stamatovic SM, Johnson AM, Keep RF, & Andjelkovic AV (2016). Junctional proteins of the blood-brain barrier: New insights into function and dysfunction. Tissue Barriers, 4(1), e1154641. doi:10.1080/21688370.2016.1154641 [PubMed: 27141427]

Starnes TW, Cortesio CL, & Huttenlocher A (2011). Imaging podosome dynamics and matrix degradation. Methods Mol Biol, 769, 111–136. doi:10.1007/978-1-61779-207-6_9 [PubMed: 21748673]

Sukriti S, Tauseef M, Yazbeck P, & Mehta D (2014). Mechanisms regulating endothelial permeability. Pulm Circ, 4(4), 535–551. doi:10.1086/677356 [PubMed: 25610592]

Tehrani S, Tomasevic N, Weed S, Sakowicz R, & Cooper JA (2007). Src phosphorylation of cortactin enhances actin assembly. Proc Natl Acad Sci U S A, 104(29), 11933–11938. doi:10.1073/pnas.0701077104 [PubMed: 17606906]

Umeda K, Ikenouchi J, Katahira-Tayama S, Furuse K, Sasaki H, Nakayama M, … Tsukita S (2006). ZO-1 and ZO-2 independently determine where claudins are polymerized in tight-junction strand formation. Cell, 126(4), 741–754. doi:10.1016/j.cell.2006.06.043 [PubMed: 16923393]

Varon C, Tatin F, Moreau V, Van Obberghen-Schilling E, Fernandez-Sauze S, Reuzeau E, … Genot E (2006). Transforming growth factor beta induces rosettes of podosomes in primary aortic endothelial cells. Mol Cell Biol, 26(9), 3582–3594. doi:10.1128/MCB.26.9.3582-3594.2006 [PubMed: 16611998]

Wang F, Cao Y, Ma L, Pei H, Rausch WD, & Li H (2018). Dysfunction of Cerebrovascular Endothelial Cells: Prelude to Vascular Dementia. Front Aging Neurosci, 10, 376. doi:10.3389/fnagi.2018.00376 [PubMed: 30505270]

Wang J, Taba Y, Pang J, Yin G, Yan C, & Berk BC (2009). GIT1 mediates VEGF-induced podosome formation in endothelial cells: critical role for PLCgamma. Arterioscler Thromb Vasc Biol, 29(2), 202–208. doi:10.1161/ATVBAHA.108.174391 [PubMed: 19023093]

Wang Y, & Alexander JS (2011). Analysis of endothelial barrier function in vitro. Methods Mol Biol, 763, 253–264. doi:10.1007/978-1-61779-191-8_17 [PubMed: 21874457]

Wu J, Yang Y, Zhang J, Ji P, Du W, Jiang P, … Shi Y (2007). Domain-swapped dimerization of the second PDZ domain of ZO2 may provide a structural basis for the polymerization of claudins. J Biol Chem, 282(49), 35988–35999. doi:10.1074/jbc.M703826200 [PubMed: 17897942]

Xu J, Kausalya PJ, Phua DC, Ali SM, Hossain Z, & Hunziker W (2008). Early embryonic lethality of mice lacking ZO-2, but Not ZO-3, reveals critical and nonredundant roles for individual zonula occludens proteins in mammalian development. Mol Cell Biol, 28(5), 1669–1678. doi:10.1128/MCB.00891-07 [PubMed: 18172007]

Yamamoto R, Aoki T, Koseki H, Fukuda M, Hirose J, Tsuji K, … Narumiya S (2017). A sphingosine-1-phosphate receptor type 1 agonist, ASP4058, suppresses intracranial aneurysm through promoting endothelial integrity and blocking macrophage transmigration. Br J Pharmacol, 174(13), 2085–2101. doi:10.1111/bph.13820 [PubMed: 28409823]

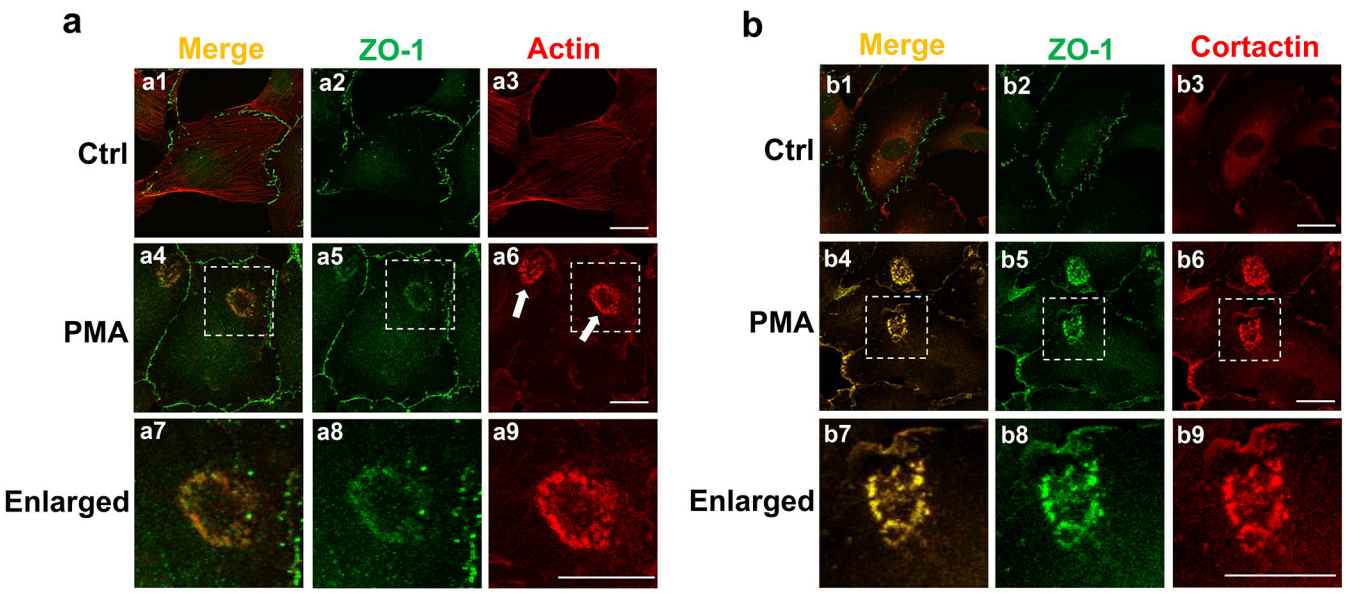

Figure 1. ZO1 localizes at podosomes in human brain endothelial cells

(**a**) Representative images of HBMECs double-stained for ZO-1 (green) and actin (red) were shown in the absence (a1-3) and presence of PMA treatment (a4-9, 100 nM for 1 hour). Enlarged pictures were shown for the white-dotted areas in a4-6, respectively. White arrows indicate the localization of podosome rosettes. Note that the merged yellow signals indicate the co-localization of ZO-1 and actin. (**b**) Co-localization of ZO-1 (green) and cortactin (red) was revealed by the similar immunostainings in HBMECs. More than 20 different cells forming podosome rosettes from at least 6 different fields (10X objective) were examined and all of them showed the co-localization of ZO-1 with actin or cortactin. n=3; scale bar: 10 μm.

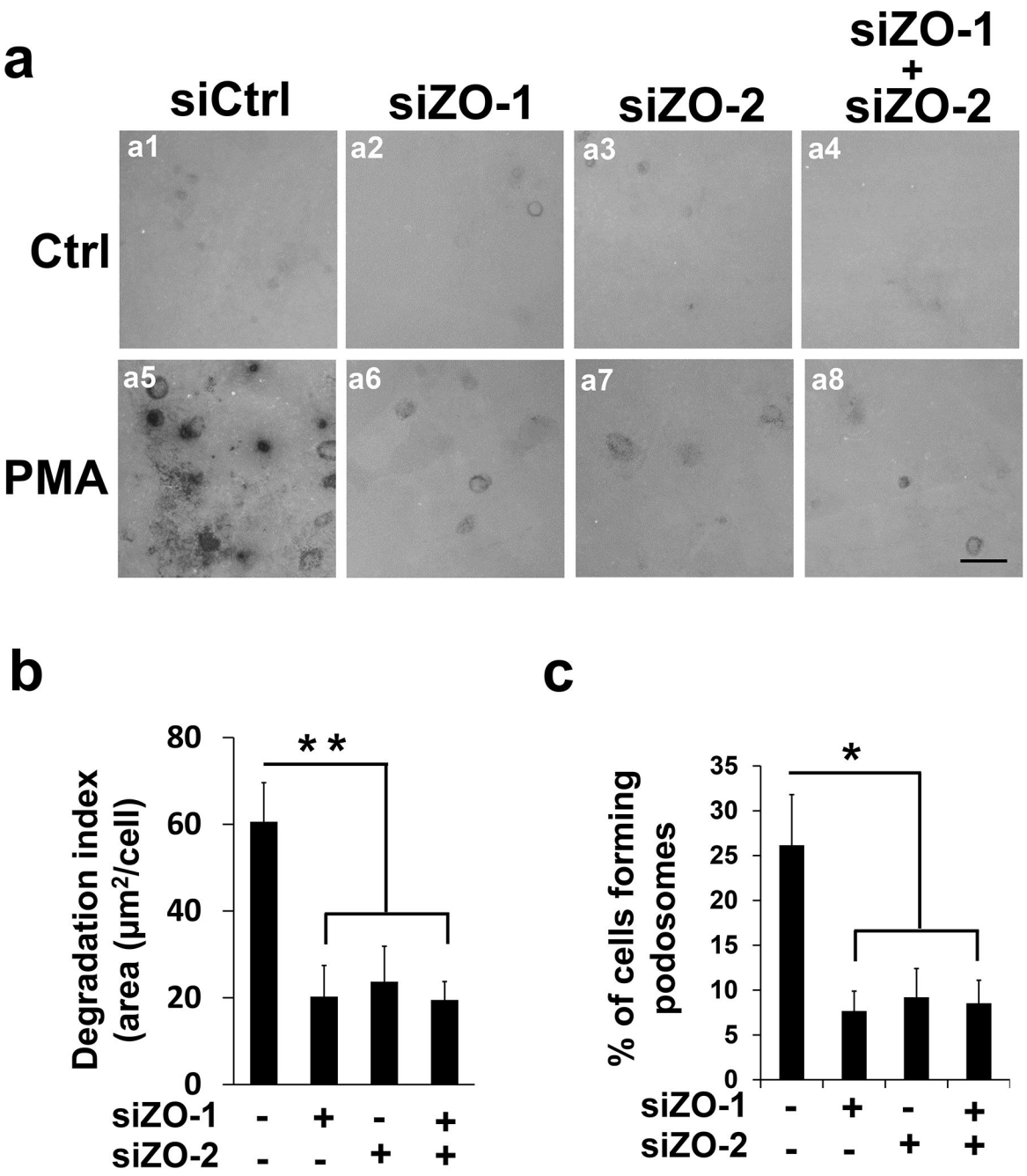

Figure 2. ZO-1 and ZO-2 are essential for podosome function in a non-redundant manner.

(**a**) SiRNAs against ZO-1 (siZO-1, 2 nM) or ZO-2 (siZO-2, 5 nM) were introduced in HBMECs singly (a2-3, and a6-7) or in combination (a4 and a8), followed by *in situ* extracellular matrix degradation assay in the absence (the first row) and presence of PMA treatment (the second row, 100 nM for 1 hour). Dark spots are caused by the loss of fluorescent signals from alexa488-labeled gelatin that was pre-coated onto the chamber slides. (**b-c**) At least 9 different fields (10X objectives) were selected to calculate the degradation index (b) and percentage of podosome formation (c) as described in Materials

and Methods. n=3; scale bar: 10 μm. Data were represented as mean±s.e.m. *p<0.05, **p<0.01.

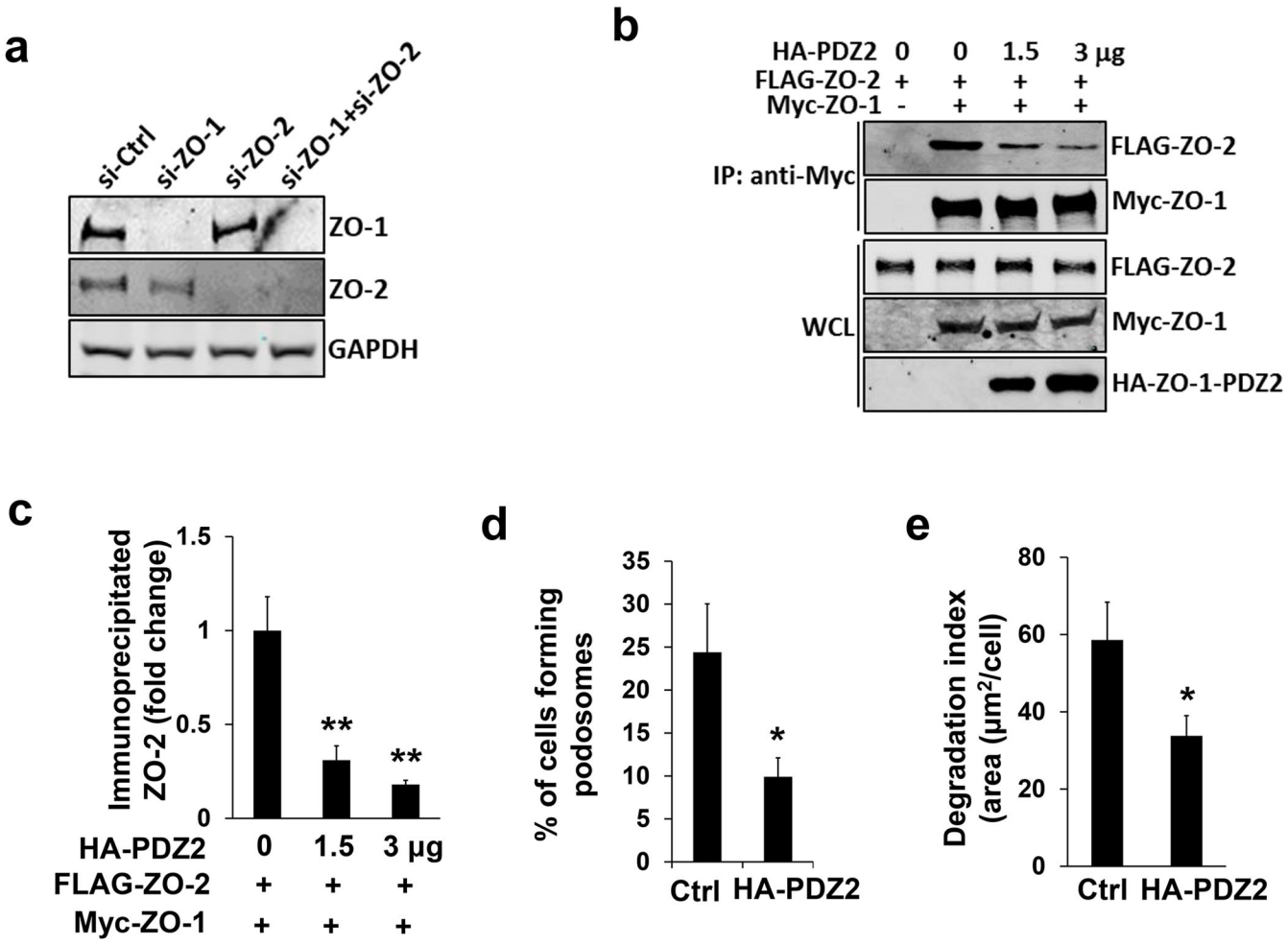

Figure 3. Dimerization of ZO-1 and ZO-2 plays an important role in podosome formation

(**a**) Single knockdown of ZO-1 (2 nM) in HBMECs does not affect protein stability of ZO-2 as revealed by Western blotting, and vice versa. GAPDH serves as loading control. (**b**) Different amount of CMV5-HA-ZO-1-PDZ2 construct (0, 1.5, 3 μg) was co-transfected with full-length FLAG-ZO-2 (1 μg) and myc-ZO-1 (1 μg) in HEK293T cells. The amount of FLAG-ZO-2 co-immunoprecipitated by the antibody against myc tag was reduced in a dose-dependent manner, which was quantified in (c) n=3. (**d-e**) Overexpression of CMV5-HA-ZO-1-PDZ2 (2 μg) in HBEMCs in the presence of PMA treatment (100 nM for 1 hour) inhibits podosome formation (d) and ECM degradation (e), n=3. HA antibody was used to highlight the transfected cells. Data were represented as mean±s.e.m, *p<0.05, **p<0.01.

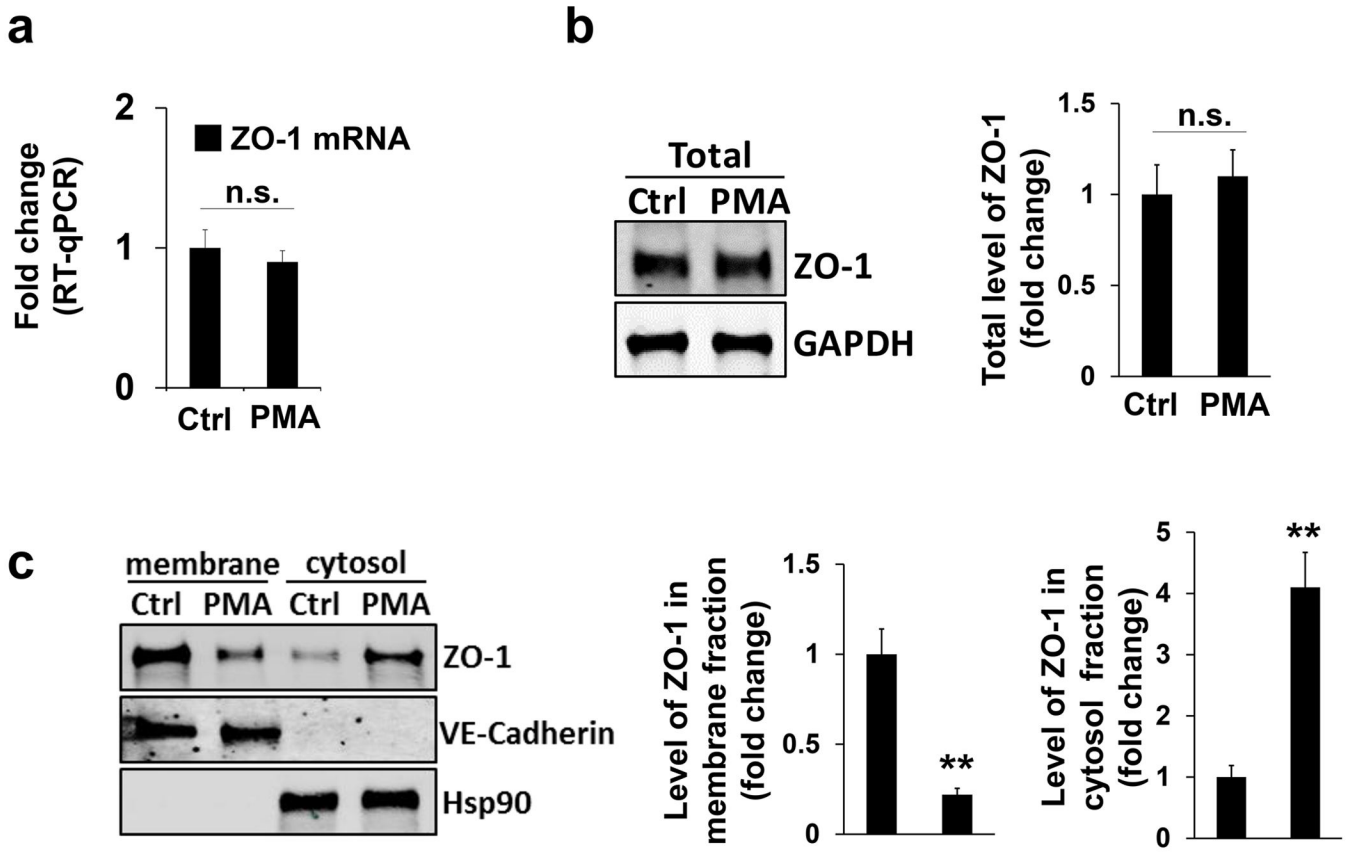

Figure 4. ZO-1 relocates from plasma membrane to podosomes

(**a-b**) Quantitative RT-PCR or Western blotting revealed the mRNA level (a) or total protein level (b) of ZO-1 in HBMECs in the absence (as indicated by Ctrl treatment (DMSO)) and presence of PMA treatment (100 nM for 1 hour). GAPDH as loading control, n=3. (**c-e**) HBMECs in the absence (Ctrl) and presence of PMA treatment were subject to membrane protein extraction assay. Western blotting showed the protein level of ZO-1 in either plasma membrane or cytosol using ZO-1 antibody, and quantifications were shown in the bar graphs. VE-cadherin as loading control for membrane fraction while Hsp90 for cytosol fraction. Data were represented as mean±s.e.m. n=3. n.s.: not significant **p<0.01.

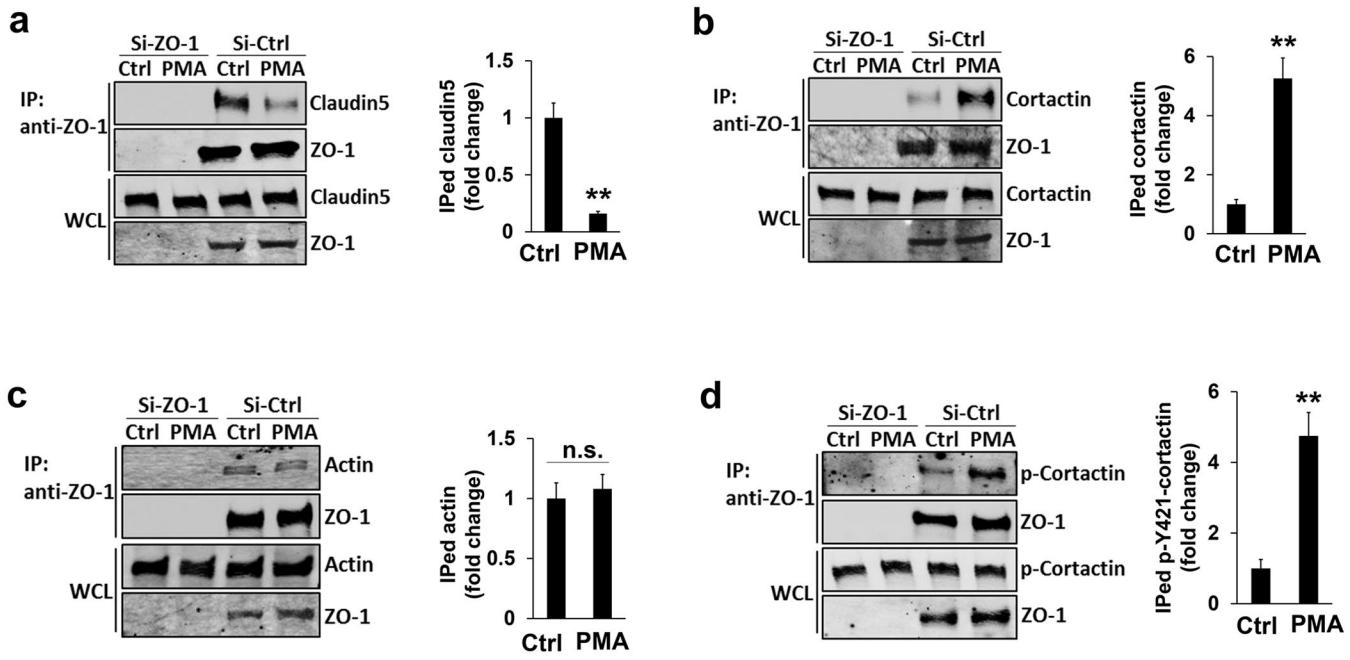

Figure 5. Enhanced interaction between ZO-1 and cortactin in response to PMA treatment.

(**a-d**) Endogenous claudin 5 (a), cortactin (b), actin (c), and phospho-Y421-cortactin (d) in HBEMCs were co-immunoprecipitated by the antibody against endogenous ZO-1 protein in the absence (DMSO) and presence of PMA treatment (100 nM for 1 hour). Western blotting revealed the protein level of each binding partner by the antibodies against claudin 5, actin, cortactin, and phosphor-Y421-cortactin, respectively. Note that the total protein level of each binding partner (the third row in a-d) remained unchanged after PMA treatment. The level of co-immunoprecipiated proteins were normalized to immunoprecipiated ZO-1 and quantified in the right panel, respectively. n=3, data were represented as mean ± s.e.m. n.s.: not significant. **p<0.01.

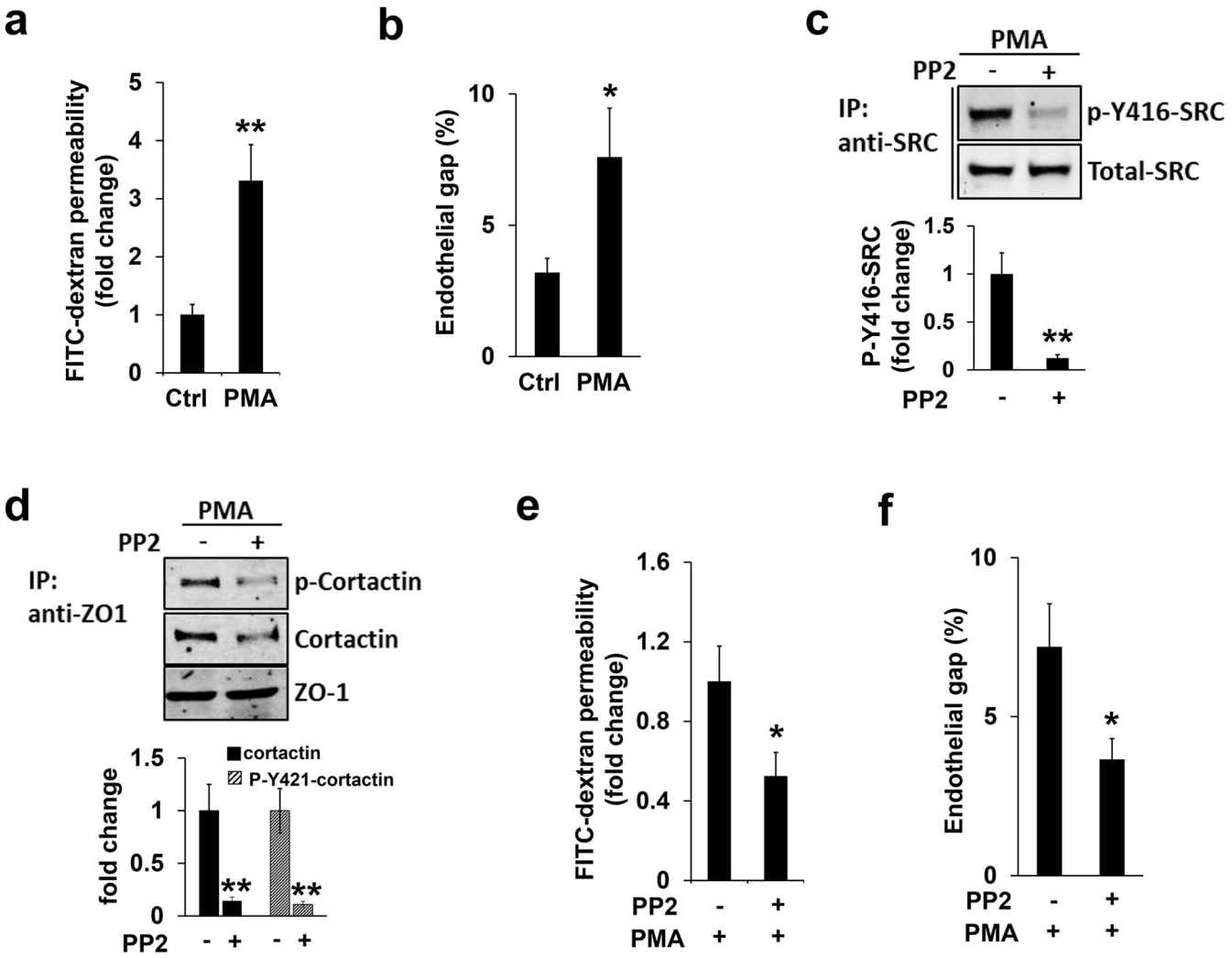

Figure 6. SRC kinase inhibition ameliorates PMA-induced endothelial barrier defect

(**a-b**) FITC-dextran permeability assay (a) or endothelial gap formation assay (b) were applied to HMBECs in the absence (DMSO) and presence of PMA treatment, as described in Materials and Methods. Note that PMA treatment significantly induced endothelial barrier leakiness. (**c-d**) HBMECs pre-incubated with PP2 (10 μM, 1 hour) or DMSO (Ctrl) were further stimulated by PMA treatment (100 nM, 1 hour). Western blotting revealed that the level of p-Y416-SRC (c) or cortactin and p-Y421-cortactin co-immunoprecipitated by ZO-1 (d) was reduced, respectively. Total protein level of SRC or immunoprecipitated ZO-1 as loading control as indicated, and quantifications were shown in the bar graphs on the bottom (**e-f**). Inhibition of SRC kinase by PP2 treatment further attenuated PMA-induced endothelial barrier defects judged by the FITC-dextran permeability assay (e) and endothelial gap formation assay (f), respectively.

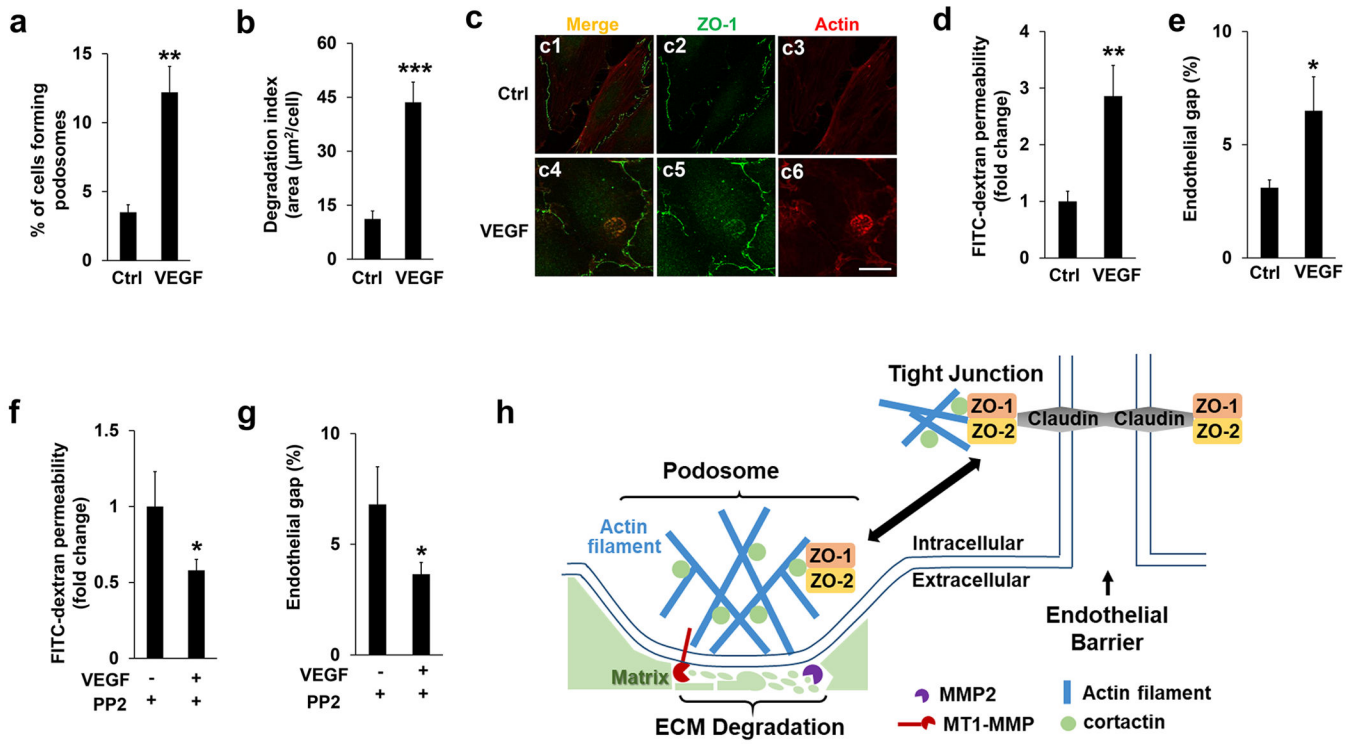

Figure 7. VEGF treatment regulates podosomal ZO proteins and endothelial barrier function.

(**a-b**) VEGF (50 ng/ml) were added to HBMECs for 1 hour, followed by podosome formation and ECM degradation assay as described previously. At least 9 different fields (10X objectives) were selected to calculate the percentage of podosomes formation (a) and the index of ECM degradation (b) as described previously. n=3. (**c**) HBMECs were immunostained by both ZO-1 and Actin antibodies in the absence (DMSO) and presence of VEGF (50 ng/ml, 1 hour). Note that VEGF treatment induced the podosomal localization of ZO-1 judged by the merged signals in c6. At least 6 different fields were selected (10 X objectives) and the podosomal ZO-1 were detected in all the cells that display podosomes, n=3. Scale bar: 10 μm. (**d-e**) FITC-dextran permeability assay (d) or endothelial gap formation assay (e) were applied to HMBECs in the absence (DMSO) and presence of VEGF (50 ng/ml, 1 hour). Note that VEGF treatment significantly induced endothelial barrier leakiness. (**f-g**) HBMECs pre-incubated with PP2 (10 μM, 1 hour) or DMSO (Ctrl) were further stimulated by VEGF treatment. Inhibition of SRC kinase by PP2 treatment further attenuated VEGF-induced endothelial barrier defects as monitored by the FITC-dextran permeability (f) and endothelial gap assay (g), respectively. n=3, *p<0.05, **p<0.01, ***p<0.01. (**h**) A schematic model for the role of ZO-1/2 in the cross-talk between podosomes and tight junctions in endothelial cells.